ACS APPLIED MATERIALS & INTERFACES

RESEARCH ARTICLE

www.acsami.org

Efficient Phosphorescent Polymer Yellow-Light-Emitting Diodes Based on Solution-Processed Small Molecular Electron Transporting Layer

Tengling Ye, Shiyang Shao, Jiangshan Chen, Lixiang Wang, and Dongge Ma*

State Key Laboratory of Polymer Physics and Chemistry, Changchun Institute of Applied Chemistry, Chinese Academy of Sciences, Graduate School of Chinese Academy of Sciences, Changchun 130022, P. R. China

ABSTRACT: Based on a solution-processed small molecular elec tron transporting layer, efficient multilayer solution-processed polymer yellow-light-emitting diodes were successfully fabricated. The maximum luminance efficiency and power efficiency reached 41.7 cd/A and 12.5 lm/W, respectively, which are comparable to and even over those from the PLEDs based on the vacuum-deposited electron-transporting layer. The solution-processed small molecular electron transporting layer is based on a mixture of three electron-transporting materials TmPyPB, TAZ, and TPBI. By utilization of this mixed system, not only the thickness of the electron-transporting layer can be easily adjusted, but also device efficiency can be improved because of their excellent synthetic properties.

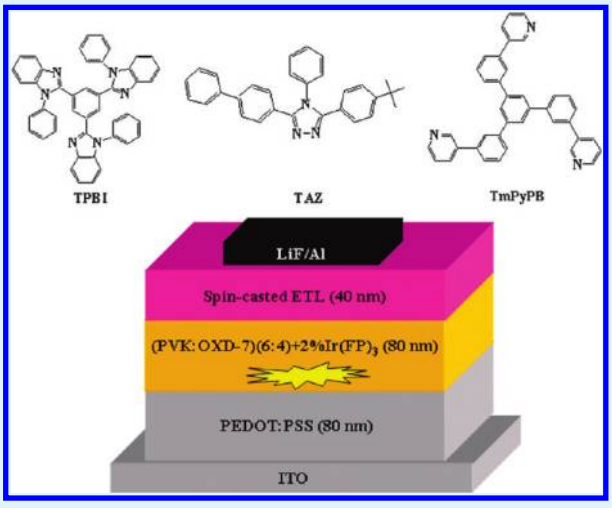

KEYWORDS: solution processed, phosphorescence, multilayer PLEDs, small molecular electron transporting layer

INTRODUCTION

Polymer light-emitting diodes (PLEDs) have attracted continuous research interests for twenty years due to their low-cost manufacturing technology, the easy-processability over large-area size, and the compatibility with flexible substrates.[1−4] However, because of the requirement of spin-symmetry conservation, the internal quantum efficiency of PLEDs based on fluorescent polymers is limited to 25%. Phosphorescent PLEDs can achieve higher quantum efficiency by harvesting near 100% energy from both singlet and triplet excitons.[5−7] Recently, the performance of phosphorescent PLEDs has been improved dramatically because of the great progresses in the aspect of both materials and device engineering.[8−10] Among these progresses, the multilayered structures are particularly inviting. Several hole-transport materials and polar solvent soluble polymers are synthesized and used to fabricate multilayer structure PLEDs.[11−23] Due to the introduction of the functional layers, the imbalanced charge transport can be adjusted and then highly efficient PLEDs can be realized. In fact, the multilayer structures are quite mature in the field of organic light emitting diodes (OLEDs) benefiting from the vacuum deposition methods.[24,25] Lots of highly efficient charge transport materials have been reported. The synthesis and purification of these small molecules are easier than those of polymers. If these efficient small molecular charge transport materials can be applied to PLEDs by solution process, it would be great benefits to improve the efficiency of PLEDs. However, the utilization of small organic transport materials in the fabrication of multilayer PLEDs is still relatively difficult due to their poor film-forming ability and dissolved problem between organic layers, where the solvent has to be orthographic to avoid this. The poor solubility of the small molecules in water−methanol mixed solvent, which is often used in multilayer phosphorescent PLEDs, greatly limits the thickness of the functional layer and thus affects device performance further.[26−28]

In this paper, we solved the thickness limitation and film-forming ability existing in the small molecule electron transport material by mixing three kinds of electron-transporting molecules together. Electron-transporting and hole-blocking properties are also greatly improved by such mixing. Hence, efficient phosphorescent yellow PLEDs were successfully fabricated. The maximum luminance efficiency and power efficiency reached 41.7 cd/A and 12.5 lm/W respectively, which are comparable to and even greater than those from the PLEDs based on vacuum-deposited electron-transporting layer.

Received: October 16, 2010
Accepted: January 17, 2011
Published: February 7, 2011

dx.doi.org/10.1021/am1010018 | *ACS Appl. Mater. Interfaces* 2011, 3, 410–416

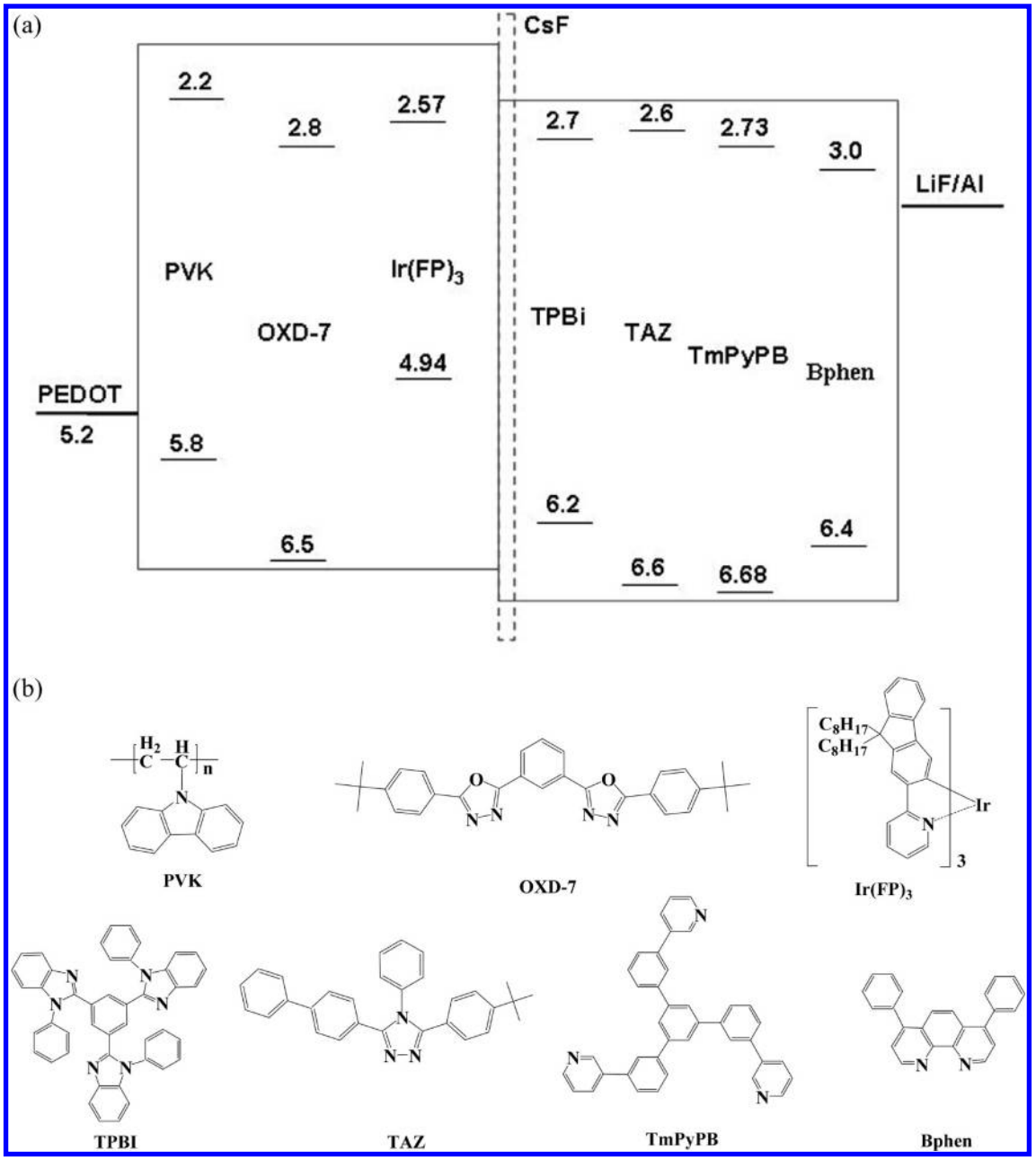

Figure 1. (a) Device structures and energy diagrams used in this study. (b) Molecular structures of the used materials.

EXPERIMENTAL SECTION

Materials. the complex reported in this work ($Ir(FP)_3$) was synthesized by ourselves from $IrCl_3.3H_2O$ and 2-(9,9-dioctyl-9*H*-fluoren-2-yl)pyridine according to a selective low-temperature syntheses method for facial tris-cyclometalated Iridium(III) complex.[29] PEDOT:PSS (Baytron P VP CH 8000) was obtained from Bayer AG, H. C. Stark, Inc. PVK was purchased from Aldrich. OXD-7 was purchased from Lumtec. Corp. All materials were used as received.

Device Fabrication. first, a 50 nm thick layer of PEDOT:PSS mixture was spin-coated on top of oxygen plasma treated indium tin oxide (ITO). This coated PEDOT on substrate was baked at 120°C in a vacuum oven for 30 minute to extract residual water. And then, the emitting layer (EML), consisting of PVK:OXD-7(60:40 weight/weight): 2 wt % $Ir(FP)_3$ was dissolved in chlorobenzene:chloroform (1:1 volume/volume) and spin-coated onto PEDOT:PSS. The samples were annealed in the vacuum oven at 120°C for 30 min to remove residual solvent. The electron-transporting/hole-blocking (ET/HB) layer was deposited either by spin-coating or by vacuum evaporation. All of the spin coated small molecular materials using in the ET/HB layer were dissolved into a mixed solvent (H_2O:MeOH 1:3 volume/volume). The concentrations of the small molecular solutions are 2 mg/mL TPBI, (1 mg of TPBI + 1 mg of TmPyPB)/mL, (1 mg of TPBI + 1 mg of TAZ)/mL, (1 mg of TPBI + 1 mg of Bphen)/mL and (1.3 mg of TPBI + 0.7 mg of TmPyPB + 1 mg of TAZ) /mL, respectively. Finally, after annealing in the vacuum oven at 120°C for 30 minutes, the LiF (1 nm) /Al (100 nm) or CsF (2 nm) /Al (100 nm) were thermally deposited as a cathode. For the single-carrier devices, the MoO_3 (10 nm) and Au(10 nm)/Al(60 nm) were thermally deposited under high vacuum. The Cs_2CO_3 interlayer was spin-coated on the ITO using ethoxy ethanol as the solvent with a concentration of 5 mg/mL and the EML was spin-coated upon the Cs_2CO_3 directly after deposition. All the solutions were filtered using

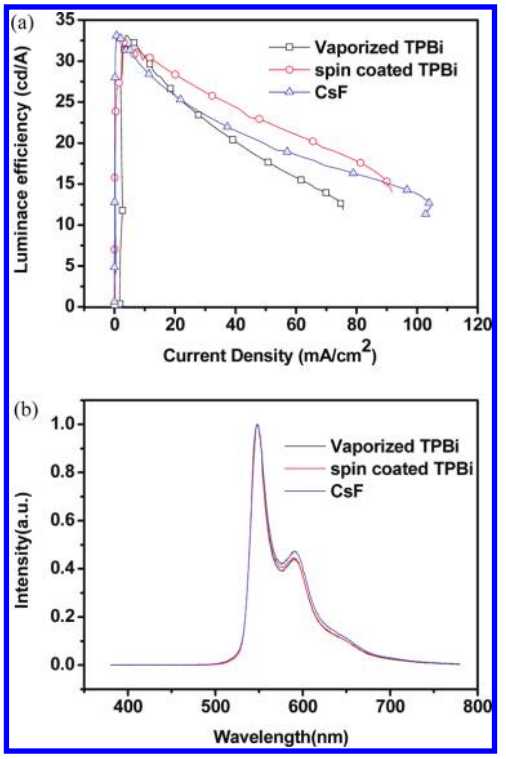

Figure 2. (a) LE−*J* for the devices ITO/PEDOT: PSS(80 nm)/EML(80 nm)/cathode (vaporized TPBI (15 nm)/LiF(1 nm)/Al, spin-coated TPBI (15 nm)/LiF(1 nm)/Al, and CsF(2 nm)/Al). (b) EL spectra of the three devices.

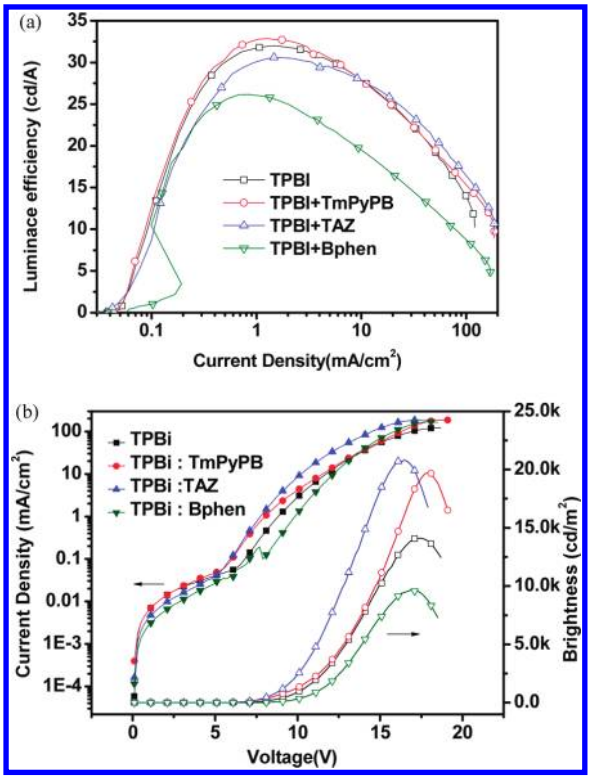

Figure 3. (a) LE−*J* for the devices ITO/PEDOT: PSS (80 nm)/EML(80 nm)/spin coated ET/HB layer(15 nm)/LiF(1 nm)/Al. The ET/HB layers are TPBI (2:0, I), TPBI:TmPyPB (1:1, II), TPBI:TAZ (1:1, III) and TPBI:Bphen (1:1, IV) in the H_2O: MeOH (1:3, v/v), respectively. (b) *J*−*B*−*V* characteristics of corresponding devices.

0.22 μm filter membranes before spin-coating. The vacuum was $<10^{-4}$ pa. The device area was 16 mm^2. The entire device fabrication was carried out outside the glove box except for the spin-coated process of EML.

Measurements. The thickness of evaporated films were monitored by frequency counter, and calibrated by Dektak 6M Profiler (Veeco). The thicknesses of spin-coated films were controlled by Dektak 6M Profiler (Veeco) directly. The EL spectra were measured by a JY SPEX CCD3000 spectrometer. Current-voltage-brightness characteristics were measured by using a Keithley source measurement unit (Keithley 2400 and Keithley 2000) with a calibrated silicon photodiode. AFM studies were carried out directly on the devices after EL performance measurement. The entire device testing was carried out in ambient atmosphere.

RESULTS AND DISCUSSION

Figure 1 shows device structures and energy diagrams used in this study.[30−32] Two types of devices are fabricated as follows:

A ITO/PEDOT:PSS/EML/CsF/Al

B ITO/PEDOT:PSS/EML/ET/HB layer/LiF/Al

PEDOT:PSS is used as both hole injecting and transporting layer. A blend consisting of poly(N-vinylcarbazole) (PVK), 1,3-bis[2-(4-tert-butylphenyl)-1,3,4-oxadiazo- 5-yl]benzene (OXD-7) and tris[2-(9,9-dioctyl-9H-fluoren-2-yl)pyridinato-C3,N] -iridium(III) $Ir(FP)_3$ is used as emitting layer (EML). TPBI, TmPyPB, TAZ and Bphen are used as the ET/HB layer. The chemical structures of the relevant materials are shown in Figure 1.

As we know, the film-forming ability of the constituting materials and mixed solvent are indispensable for the multilayer phosphorescent PLEDs based on all solution process. Fortunately, as a very typical small molecular electron-transporting material, we find that TPBI can be dissolved in the classical mixed solvent (H_2O:MeOH, 1:3) and form high quality film. We successfully fabricate multilayer phosphorescent PLEDs based on solution-processed TPBI as ET/HB layer. Figure 2a shows the luminance efficiency (LE) versus current density (*J*) characteristics of the multilayer PLEDs with different systems (vaporized TPBI/LiF/Al, spin coated TPBI/LiF/Al and CsF/Al). It can be seen that the spin coated TPBI electron-transporting layer exhibits approximate luminance efficiency (32.3 cd/A) as that of vaporized TPBI electron-transporting layer (33.2 cd/A) and CsF interlayer (33.3 cd/A). In Figure 2b, all devices exhibit nearly the same light emission at 548 nm, which is from $Ir(FP)_3$ dopant. The processing method of TPBI layer does not affect the emitting color of the multilayer PLEDs. These results clearly indicate that the solution-processed TPBI film can play the same role as the corresponding vacuum-processed TPBI film and CsF. However, the solubility of TPBI in the mixed solvent (H_2O:MeOH, 1:3) isn't so good at higher doping concentration, thus the thickness of TPBI layer is difficult to be over 15 nm by spin-coating. In other words, it is impossible to further optimize the device performance by adjusting the thickness of TPBI layer via spin-coating.

Actually, we have tried to use TmPyPB, TAZ, and Bphen instead of TPBI as the ET/HB layer to solve the thickness problem. Unfortunately, the results are not expected by us. The thickness can not be solved by a single component. Thereupon, we think of the concept of additive solubility property of inorganic salt, can it extend to our system? Excitingly, we find

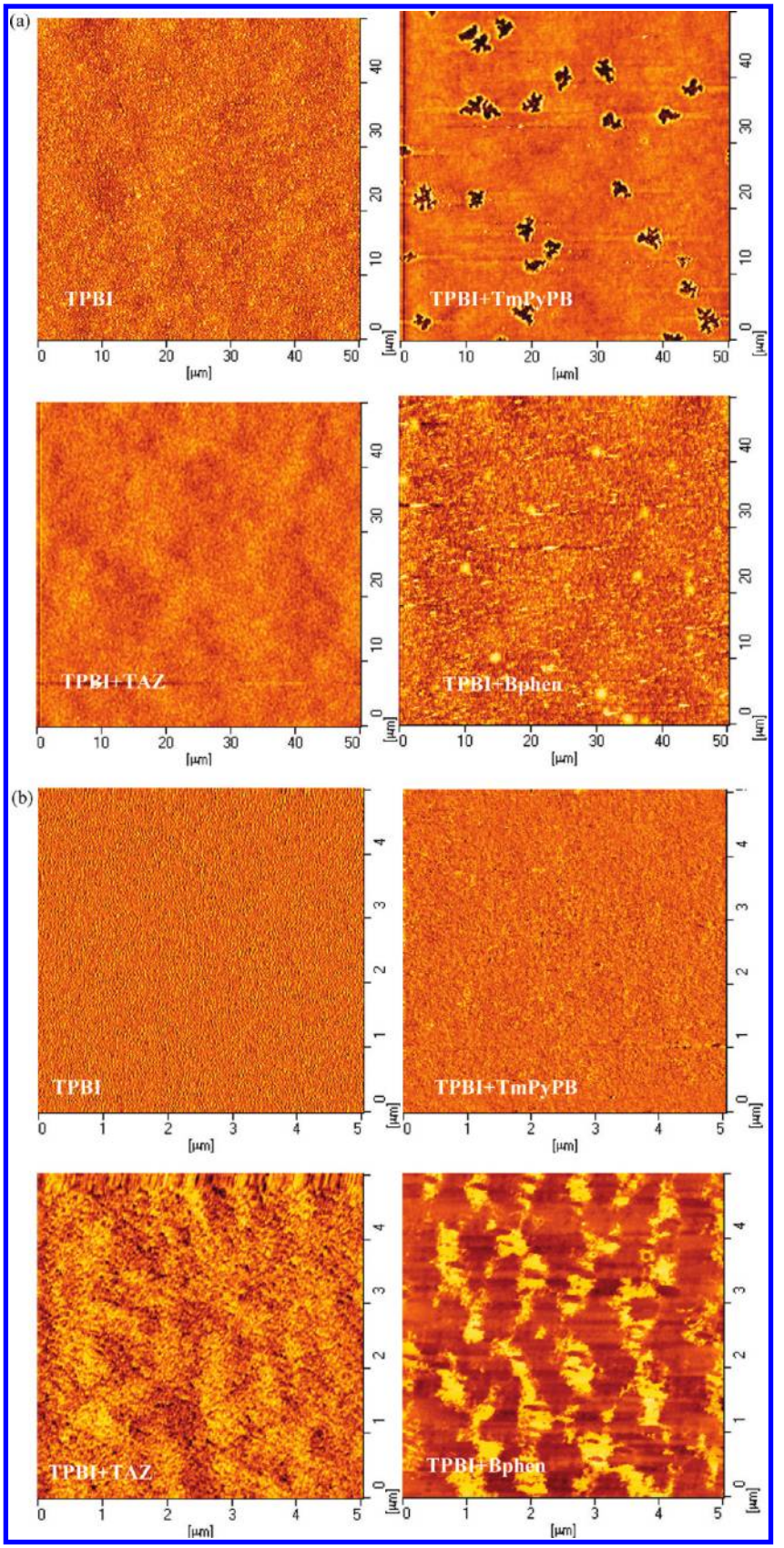

Figure 4. (a) AFM surface morphology images (50 μm) of the devices coated with different ET/HB layers: TPBI (2:0, I), TPBI:TmPyPB (1:1, II), TPBI:TAZ (1:1, III), and TPBI:Bphen (1:1, IV) in the H_2O:MeOH (1:3, v/v), respectively. (b) AFM phase images (5μm) of corresponding devices.

Table 1. Comparison of Properties of Four Film Systems

components	TPBI	TPBI+TmPyPB	TPBI+TAZ	TPBI+Bphen
solubility in mixed solvent	mid-level	poor	good	good
phase uniform	good	very good	good	poor
film continuity	good	poor	good	good
energy-match (LUMO)	good	good	good	poor
hole block ability (HOMO)	poor	very good	very good	good
mobility	low[a]	very high[b]	very low[c]	high[d]
device performance	better	best	good	poor

[a] The electron mobility of vacuum deposited TPBI film is $(3.3-8) \times 10^{-5}$ (cm^2/V s) at a field strength of $(4.7-7) \times 10^5$ V/cm.[33] [b] The electron mobility of vacuum deposited TmPyPB film is $(7-10) \times 10^{-4}$ (cm^2/V s) at a field strength of $(2.5-6.4) \times 10^5$ V/cm.[32] [c] The electron mobility of vacuum deposited TAZ film is $(1-3) \times 10^{-5}$ (cm^2/V s) at a field strength of $(4.2-6.7) \times 10^5$ V/cm.[34] [d] The electron mobility of vacuum deposited Bphen film is $\sim 3 \times 10^{-4}$ (cm^2/V s) at a field strength of $\sim 4.9 \times 10^5$ V/cm.[35]

that mixing three kinds of proper electron-transporting molecules together can well-adjust the thickness of ET/HB layer. To optimize the material systems, we first studied the two-component mixture of TPBI, TPBI:TmPyPB, TPBI:TAZ, and TPBI:Bphen. As we know, TmPyPB, TAZ, and Bphen are also widely used electron-transporting materials in OLEDs, which show proper lowest unoccupied molecular orbital (LUMO), much higher highest occupied molecular orbital (HOMO) and higher electron mobility. We fabricated four devices based on TPBI (2:0, I), TPBI:TmPyPB (1:1, II), TPBI:TAZ (1:1, III) and TPBI:Bphen (1:1, IV), which were dissolved in water/methanol (1:3, v/v) solvent mixtures. Panels a and b in Figure 3 show the corresponding luminance efficiency versus current density and current density−brightness−voltage characteristics of the four devices. Except for device IV, which shows high operational voltage, low brightness, and low LE, devices II and III exhibit similar LE to device I. The difference is that the operational voltage is reduced and the brightness is greatly enhanced in devices II and III.

To explain the above results, we check the microscopic morphologies of TPBI (I), TPBI:TmPyPB (II), TPBI:TAZ (III), and TPBI:Bphen (IV) films by atomic force microscope (AFM). Images a and b in Figure 4 show the corresponding AFM surface morphology images (50 μm) and phase images (5 μm), respectively. From Figure 4a, it can be found that the films (I, III, and IV) are continuous except that the film II has slight pin holes. In addition, the roughness of the films (I, II, III, and IV) is 1.805, 0.4448, 0.4986, and 1.398 nm in the morphology images (5 μm), respectively. These results indicate that both TmPyPB and TAZ can flatten the surface of TPBI film, which should be favorable to enhance the performances of PLEDs. Figure 4b gives the phase images (5 μm) of the films (I, II, III, and IV). It can be seen that the phase separation doesn't take place in the films (I, II, and III) except for the film IV. This indicates that TPBI:Bphen film is easily crystallized, which leads to the low performance. It is concluded that TPBI:Bphen film is not suitable as ET/HB layer.

The merits and drawbacks of the four systems are summarized in the Table 1. As we can see, by introducing TmPyPB or TAZ into TPBI, the operational voltage can be reduced and the brightness can be enhanced. The ET/HB layer thickness can be increased. However, this isn't the optimized results because the ET/HB layer thickness still can't reach the value we expect. Thus, we attempt to mix three components together. On basis of synthetically considering, we mixed TmPyPB and TAZ together into TPBI as ET/HB layer. The optimized mixture ratio is TPBI:TmPyPB:TAZ =1.3:0.7:1. As expected, the ET/HB layer thickness is easy to increase to 40 nm and the efficiency of the PLEDs is further improved. Panels a and b in Figure 5 compare the EL performance of the devices based on TPBI:TmPyPB:TAZ as the ET/HB layer with different thicknesses and the control device using vaporized TPBI as ET/HB layer with 40 nm thickness. Besides that the operational voltage is reduced, the LE is also enhanced in device with 40 nm spin-coated TPBI:TmPyPB:TAZ as the ET/HB layer compared to the device with 40 nm vaporized TBPi as the ET/HB layer. The maximum LE and external quantum efficiency reached 41.7 cdA^{-1} and 12.7%. The maximum brightness is 23926 cd m^{-2}.

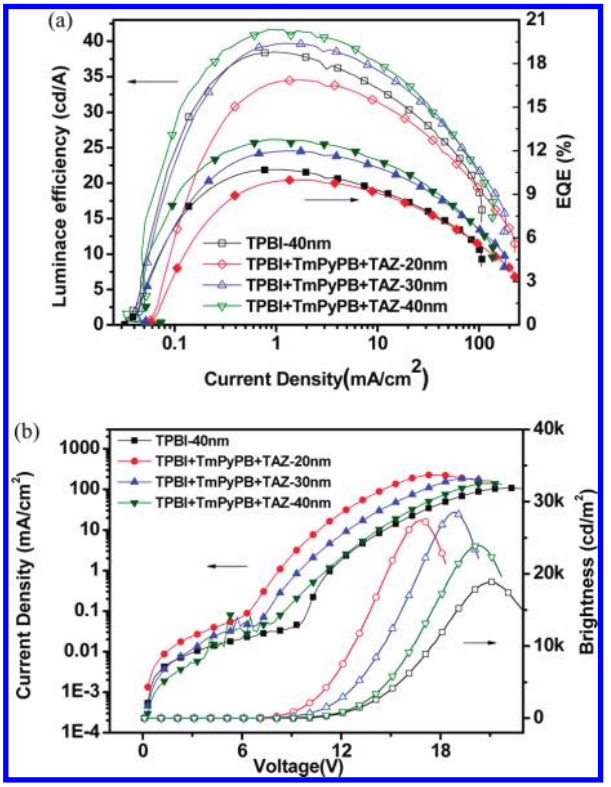

Figure 5. (a) LE−*J* for the devices ITO/PEDOT:PSS(80 nm)/EML-(80 nm)/ET/HB layer/LiF(1 nm)/Al. The ET/HB layers are TPBI:TmPyPB:TAZ (20 nm), TPBI:TmPyPB:TAZ (30 nm), TPBI:TmPyPB:TAZ (40 nm) in the H_2O:MeOH (1:3, v/v), and vaporized TPBI (40 nm), respectively. (b) *V*−*J*−*B* characteristics of corresponding devices.

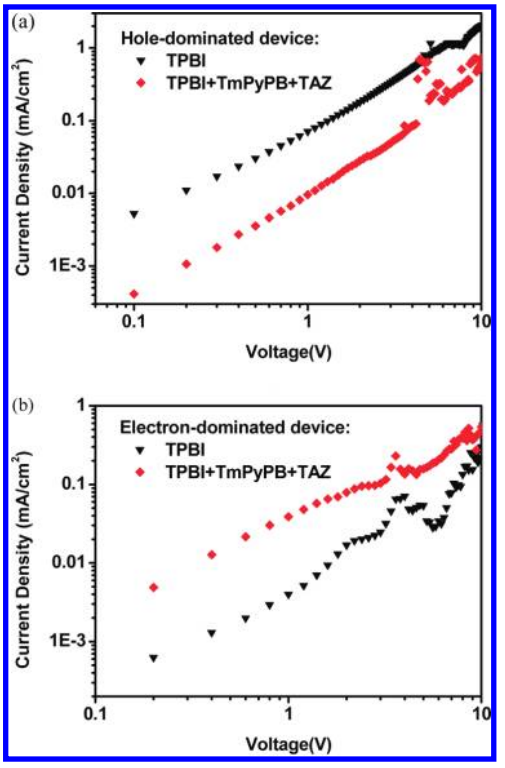

Figure 6. $J-V$ characteristics of the single-carrier devices coated with different ET/HB layers: TPBI:TmPyPB:TAZ (40 nm) in the H_2O:MeOH (1:3, v/v) and vaporized TPBI (40 nm), respectively. (a) Hole-dominated device and (b) the electron-dominated device.

To demonstrate the improvement possibility in device performance, two kinds of single-carrier devices are fabricated as follows

(a) The hole-dominated device:
- ITO/PEDOT:PSS(80 nm)/EML(80 nm)/TPBI + TmPyPB + TAZ (40 nm, spin coated)/MoO_3(10 nm)/Au(10 nm)/Al(60 nm)
- ITO/PEDOT:PSS(80 nm)/EML(80 nm)/TPBI (40 nm, vaporized)/MoO_3(10 nm)/Au(10 nm)/Al(60 nm)

(b) The electron-dominated device:
- ITO/Cs_2CO_3(2 nm)/EML(80 nm)/TPBI + TmPyPB + TAZ (40 nm, spin coated)/LiF(1 nm)/Al (100 nm)
- ITO/Cs_2CO_3(2 nm)/EML(80 nm)/TPBI (40 nm, vaporized)/LiF(1 nm)/Al (100 nm)

As shown in panels a and b in Figure 6, compared with the control devices with vaporized TBPi as the ET/HB layer, the hole current density of the device with spin-coated TPBI:TmPyPB:TAZ as the ET/HB layer is reduced, whereas the electron current density of the device with spin-coated TPBI:TmPyPB:TAZ as the ET/HB layer is enhanced. This indicates that the introduction of TmPyPB and TAZ strengthens the hole-blocking ability and also improves the electron injection and transport of ET/HB layer at the same time. The performance enhancement can be attributed to the better comprehensive properties of the TPBI:TmPyPB:TAZ film. The higher HOMO energy levels of the TmPyPB and TAZ make the block of holes and excitons more efficient. The multifold LUMO energy levels and the higher electron mobility of TmPyPB make electron injection and transport easier.

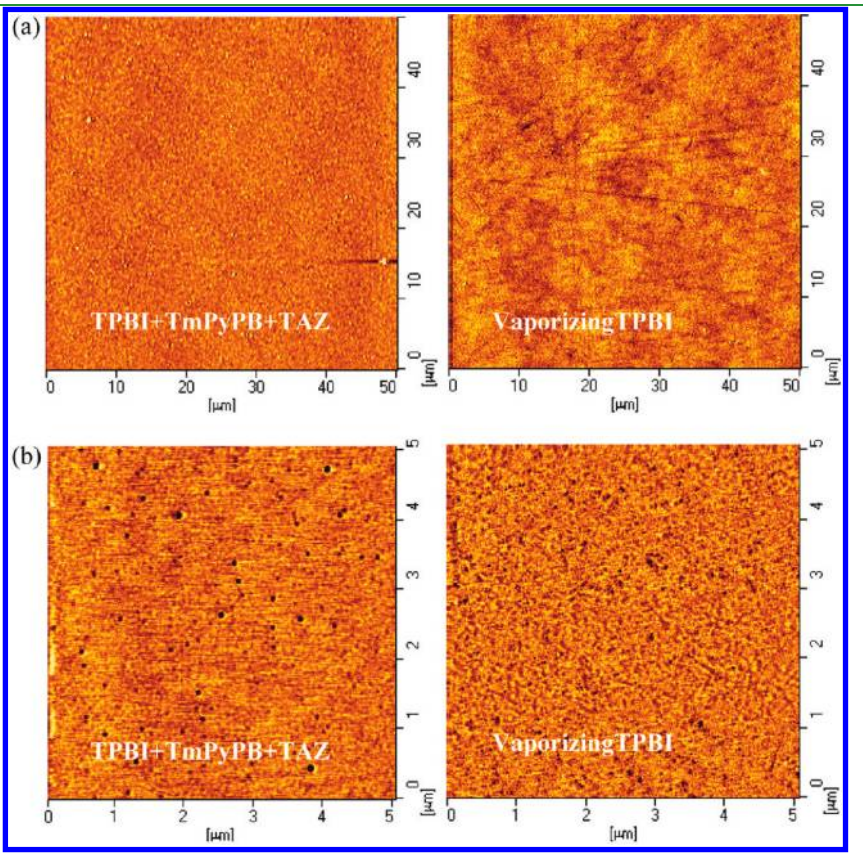

Figure 7. (a) AFM surface morphology images (50 μm) of the devices coated with different ET/HB layers: TPBI:TmPyPB:TAZ (40 nm) in the H2O:MeOH (1:3, v/v) and vaporized TPBI (40 nm), respectively. (b) AFM phase images (5 μm) of corresponding devices.

To further show the merit of our concept, we also compared the microscopic morphologies of the spin-coated TPBI: TmPyPB:TAZ films with the vaporized TPBI film. Images a and b in Figure 7 how the corresponding AFM surface morphology images and phase images in different scales (50 and 5 μm, respectively). From the surface morphology images in a large scale of 50 μm, we can find that both of material systems show continuous films without any pin holes. In the scale of 5 μm, the roughness of the spin-coated TPBI: TmPyPB: TAZ film and the vaporized TPBI film is 0.839 nm, and 0.481 nm, respectively, and the phase separation is not also observed in TPBI:TmPyPB:TAZ film. These results indicate that TPBI:TmPyPB:TAZ is good material system as ET/HB layer for fabricating high-efficiency solution-processed phosphorescent PLEDs.

CONCLUSIONS

In conclusion, we have successfully fabricated high efficiency phosphorescent polymer yellow-light-emitting diodes based on solution-processed small molecular electron transporting layer. The solution-processed small molecular electron transporting layer is based on the mixture of three electron-transporting materials TmPyPB, TAZ, and TPBI. We found that the choice of proper three electron-transporting materials can not only easily adjust the thickness of the electron-transporting layer, but also greatly improve device performance because of the synthetic properties of good film morphology, good electron transport, and effective hole blocking role of the mixed system. The maximum luminance efficiency and power efficiency, respectively, reached 41.7 cd/A and 12.5 lm/W, which are comparable to and even over those from the PLEDs based on vacuum-deposited electron-transporting layer. We expect the approach to form solution-processed electron-transporting layer demonstrated here for high efficiency yellow phosphorescent PLEDs to be also applicable to green, red, blue, and white multilayer PLEDs.

AUTHOR INFORMATION

Corresponding Author
*E-mail: mdg1014@ciac.jl.cn.

ACKNOWLEDGMENT

The authors thank the Science Fund for Creative Research Groups of NSFC (20921061), the National Natural Science Foundation of China (50973104, 60906020), Ministry of Science and Technology of China (973 Program 2009CB623604, 2009CB930603), the Foundation of Jilin Research Council (20080337, 20090127) for the support of this research.

REFERENCES

(1) Braun, D.; Heeger, A. J. *Appl. Phys. Lett.* **1991**, *58*, 1982.
(2) Gong, X.; Ma, W.; Ostrowski, J. C.; Bazan, G. C.; Moses, D.; Heeger, A. J. *Adv. Mater.* **2004**, *16*, 615.
(3) Gong, X.; Wang, S.; Moses, D.; Bazan, G. C.; Heeger, A. J. *Adv. Mater.* **2005**, *17*, 2053.
(4) Tu, G. L.; Mei, C. Y.; Zhou, Q. G.; Cheng, Y. X.; Geng, Y. H.; Wang, L. X.; Ma, D. G.; Jing, X. B.; Wang, F. S. *Adv. Funct. Mater.* **2006**, *16*, 101.
(5) Baldo, M. A.; O'Brien, D. F.; Thompson, M. E.; Forrest, S. R. *Phys. Rev. B.* **1999**, *60*, 14422.
(6) Adachi, C.; Baldo, M. A.; Thompson, M. E.; Forrest, S. R. *J. Appl. Phys.* **2001**, *90*, 5048.
(7) Choulis, S. A.; Mathai, M. K.; Choong, V. E.; So, F. *Appl. Phys. Lett.* **2006**, *88*, 203502.
(8) Huang, J. S.; Li, G.; Wu, E.; Xu, Q. F.; Yang, Y. *Adv. Mater.* **2006**, *18*, 114.
(9) Wu, H. B.; Zhou, G. J.; Zou, J. H.; Ho, C. L.; Wong, W. Y.; Yang, W.; Peng, J. B.; Cao, Y. *Adv. Mater.* **2009**, *21*, 4181.
(10) Ding, J. Q.; Zhang, B. H.; Lü, J. H.; Xie, Z. Y.; Wang, L. X.; Jing, X. B.; Wang, F. S. *Adv. Mater.* **2009**, *21*, 4983.
(11) Lee, T. W.; Park, O. O.; Do, L. M.; Zyung, T.; Ahn, T.; Shim, H. K. *J. Appl. Phys.* **2001**, *90*, 2128.
(12) Wu, H.; Huang, F.; Mo, Y.; Yang, W.; Wang, D.; Peng, J.; Cao, Y. *Adv. Mater.* **2004**, *16*, 1826.
(13) Yan, H.; Huang, Q. L.; Scott, B. J.; Mark, T. J. *Appl. Phys. Lett.* **2004**, *84*, 3873.
(14) Yan, H.; Lee, P.; Armstrong, N. R.; Graham, A.; Evmenenko, G. A.; Dutta, P.; Mark, T. J. *J. Am. Chem. Soc.* **2005**, *127*, 3172.
(15) Zhou, G.; Qian, G.; Ma, L.; Cheng, Y. X.; Xie, Z. Y.; Wang, L. X.; Jing, X. B.; Wang, F. S. *Macromolecules* **2005**, *38*, 5416.
(16) Huang, F.; Niu, Y. H.; Zhang, Y.; Ka, J. W.; Liu, M. S.; Jen, A. K. Y. *Adv. Mater.* **2007**, *19*, 2010.
(17) Niu, X.; Qin, C. J.; Zhang, B. H.; Yang, J. W.; Xie, Z. Y.; Cheng, Y. X.; Wang, L. X. *Appl. Phys. Lett.* **2007**, *90*, 203513.
(18) Huang, F.; Shih, P. I.; Shu, C. F.; Chi, Y.; Jen, A. K. Y. *Adv. Mater.* **2009**, *21*, 361.
(19) Oh, S. H.; Vak, D.; Na, S. I.; Lee, T. W.; Kim, D. Y. *Adv. Mater.* **2008**, *20*, 1624.
(20) Hoven, C. V.; arcia, A.; Bazan, G. C.; Nguyen, T. Q. *Adv. Mater.* **2008**, *20*, 3793.
(21) Hoven, C. V.; Yang, R.; Garcia, A.; Crockett, V.; Heeger, A. J.; Bazan, G. C.; Nguyen, T. Q. *Proc. Natl. Acad. Sci. U.S.A.* **2008**, *105*, 12730.
(22) Xu, Y. H.; Yang, R. Q.; Peng, J. B.; Mikhailovsky, A. A.; Cao, Y.; Nguyen, T. Q.; Bazan, G. C. *Adv. Mater.* **2009**, *21*, 584.
(23) Zhang, B. H.; Qin, C. J.; Ding, J. Q.; Chen, L.; Xie, Z. Y.; Cheng, Y. X.; Wang, L. X. *Adv. Mater.* **2010**, *20*, 2951.
(24) Wang, Q.; Ding, J. Q.; Ma, D. G.; Cheng, Y.; Cheng, Y. X.; Wang, L. X.; Wang, F. S. *Adv. Mater.* **2009**, *21*, 2397.
(25) Wang, Q.; Ding, J. Q.; Ma, D. G.; Cheng, Y.; Cheng, Y. X.; Wang, L. X.; Jing, X. B.; Wang, F. S. *Adv. Funct. Mater.* **2009**, *19*, 84.
(26) Lee, T. W.; Noh, T.; Shin, H. W.; Kwon, O.; Park, J. J.; Choi, B. K.; Kim, M. S.; Shin, D. W.; Kim, Y. R. *Adv. Funct. Mater.* **2009**, *19*, 1625.
(27) You, J. D.; Tseng, S. R.; Meng, H. F.; Yen, F. W.; Lin, I. F.; Horng, S. F. *Org. Electron.* **2009**, *10*, 1610.
(28) Kim, K. H.; Lee, J. Y.; Park, T. J.; Jeon, W. S.; Kennedy, G. P.; Kwon, J. H. *Synth. Met.* **2010**, *160*, 631.
(29) McGee, K. A.; Mann, K. R. *Inorg. Chem.* **2007**, *46*, 7800.
(30) Xie, W.; Wu, Z.; Hu, W.; Zhao, Y.; Li, C.; Li, S. *Semicond. Sci. Technol.* **2005**, *20*, 443.
(31) He, G.; Walzer, K.; Pfeiffer, M.; Leo, K.; Pudzich, R.; Salbeck, J. *Proc. SPIE* **2004**, *5519*, 42.
(32) Su, S. J.; Chiba, T.; Takeda, T.; Kido, J. *Adv. Mater.* **2008**, *20*, 2125.
(33) Hung, W. Y.; Ke, T. H.; Lin, Y. T.; Wu, C. C.; Hung, T. H.; Chao, T. C.; Wong, K. T.; Wu, C. I. *Appl. Phys. Lett.* **2006**, *88*, 064102.
(34) Sasabe, H.; Eisuke, G.; Chiba, T.; Li, Y. J.; Tanaka, D.; Su, S. J.; Takeda, T.; Pu, Y. J.; Nakayama, K. I.; Kido, J. *Chem. Mater.* **2008**, *20*, 5951.
(35) Naka, S.; Okada, H.; Onnagawa, H.; Tsutsui, T. *Appl. Phys. Lett.* **2000**, *76*, 197.